# STATE UNIVERSITY OF NEW YORK AT STONY BROOK



COLLEGE OF ENGINEERING

THERMODYNAMICS AND KINETICS OF REACTIONS

IN PROTECTIVE COATING SYSTEMS

B. Gupta, A. Sarkhel, R. Sivakumar, L. Seigle

Third Semiannual Report for the Period

December 1, 1973 - May 31, 1974

NASA Research Grant NGR-33-015-160

# THERMODYNAMICS AND KINETICS OF REACTIONS IN PROTECTIVE COATING SYSTEMS

B. Gupta, A. Sarkhel, R. Sivakumar, L. Seigle

Third Semiannual Report for the Period

December 1, 1973 - May 31, 1974

NASA Research Grant NGR-33-015-160

TABLE OF CONTENTS

## I. Introduction

A basic study is being made of the formation and degradation of aluminide coatings on pure Ni and Co, in order to clarify the fundamental processes which control the behavior of such "diffusion-type" coatings. This includes a careful investigation of the thermodynamics and kinetics of the pack-aluminization process, as well as a theoretical and experimental study of the degradation of aluminide coatings by interaction with the substrate. The relative importance of coating-substrate interaction and oxidation as mechanisms of coating degradation is a question also being considered. A report of progress in the various investigations made during the period December 1, 1973 - May 31, 1974 is given in the following.

## II. Boundary Conditions for Diffusion During Pack Aluminizing

As explained in previous reports,[1] the relationship of the composition of the specimen surface to the composition of the pack is a critical index in determining whether or not solid state diffusion is rate-controlling in the aluminization process. The variation of surface composition with time, temperature and pack composition is being investigated using Ni specimens in aluminum fluoride activated packs. During the last six months, effort has been devoted to obtaining data using packs with higher Al:Ni ratios and at lower temperatures. The variation of surface composition with time has been obtained in packs containing 55 - 100 a/o Al, at temperatures ranging from 800 - 1093°C. The experimental techniques were similar to those used in previous tests, except that the ratio of metal to non-metal powder in the packs was decreased for the 85 and 100 a/o Al packs, in order to avoid problems due to the formation of liquid phase at high Al:Ni ratios.

Table I presents the data obtained from packs containing 55 - 70 a/o Al. The metal-nonmetal ratio was held at 50:50 wt.% in the packs, and the packs were

activated with 4 w/o, $AlF_3$.

TABLE I

Variation of Surface Composition with Time

| Time - hrs. | Surface Composition - a/o Al | | | | | |
|---|---|---|---|---|---|---|
| | 55 a/o Al Pack | | 58 a/o Al Pack | | 70 a/o Al Pack | |
| | 1093°C | 1000°C | 1093°C | 1000°C | 900°C | 800°C |
| 2 | 46.12 | 46.28 | 47.48 | 46.02 | 53.17 | 53.31 |
| 5 | 46.79 | 46.52 | 48.22 | 47.14 | —— | 52.94 |
| 10 | 47.19 | 46.55 | 48.60 | 47.84 | 53.96 | —— |
| 20 | 47.53 | 46.99 | 48.51 | 47.99 | 54.08 | 52.95 |

It may be seen that under all conditions the surface Al concentration, reaches a high value within two hours and remains almost constant with time after this. However, as previously observed, the surface composition of these higher Al packs remains substantially below the normal pack composition. As can be seen from Fig. 1, Progress Report #2, the boundary of the NiAl phase lies at ∿ 55 a/o Al. The 58 a/o Al pack in Table I lies in the two-phase region, NiAl + $Ni_2Al_3$, and the 70 a/o Al pack in the $Ni_2Al_3$ + L region. Under equilibrium conditions it would be expected that the phase at the coating surface should be NiAl of 55 a/o Al on the specimen coated in the 58 a/o Al pack, and $Ni_2Al_3$ on the specimen in the 70 a/o Al pack. Only NiAl appears on these specimens, however, and the surface composition is less than 55 a/o Al. Since the 58 and 70 a/o Al packs lie within two-phase regions, it is difficult to argue that the discrepancy between surface and pack a/o Al is due to loss of Al from the pack. Loss of a small amount of Al would merely alter the ratio of phase amounts, without changing the activity of

Al. Therefore, it appears that an Al activity gradient must exist between the pack and the specimen surface in these high Al packs.

Fig. 1(a) illustrates the as coated appearance of a sample aluminized in 58 a/o Al pack. Well formed grains and pronounced grain boundaries are evident on a clean and bright surface. Subgrain boundaries are also visible. Figs. 1(b) and 1(c) give the appearance of the NiAl coating in 70 a/o Al pack at 1093°C and 900°C. Surface composition of these two samples lies close to the NiAl phase boundary (∿ 54 a/o Al) as opposed to surface composition of sample shown in Fig. 1(a) (48 a/o Al). The surface structure of these two samples is not easily resolvable. In Fig. 1(b), underlying grain structure is visible. These two samples have dull grey appearance, whereas NiAl of surface composition 48 a/o Al is very shiny and bright. There is no evidence of pack adherence on these two samples. NiAl (surface composition, 48 a/o Al) has bright appearance without any trace of original Ni substrate surface features. This suggested that it has been formed by predominant outward Ni diffusion. NiAl (surface composition, 54 a/o Al) appears quite different. If it were only inward Al diffusion, original scratch marks on Ni would be visible. This appearance could be due to the phase being formed by both Ni and Al diffusion.

When packs containing very high Al:Ni ratios were investigated, such as the 85 a/o Al and 100 a/o Al packs, it was found necessary to decrease the metal: filler ratio in order to minimize pack sintering, and avoid partial melting of the specimens. Initially a metal:filler ratio of 10:90 w/o was chosen for these packs, and results are tabulated in Table II.

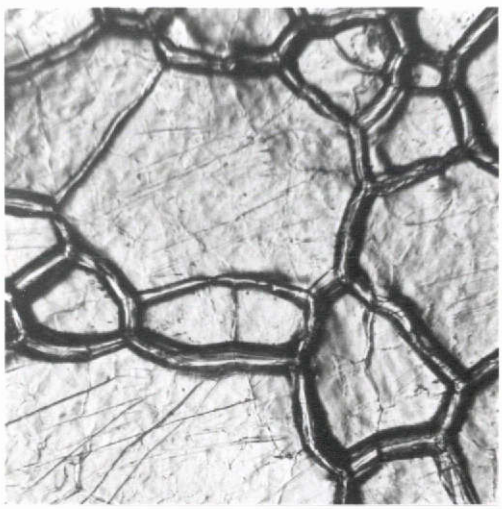

a. MICROPHOTOGRAPH, 200X
(58 a/o Al PACK, 1093°C)

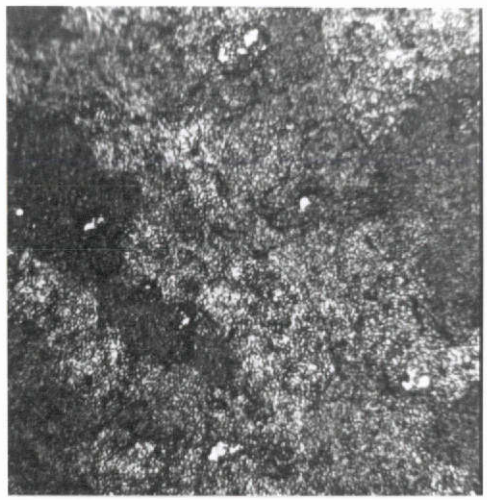

b. MICROPHOTOGRAPH, 200X
(70 a/o Al PACK, 1093°C)

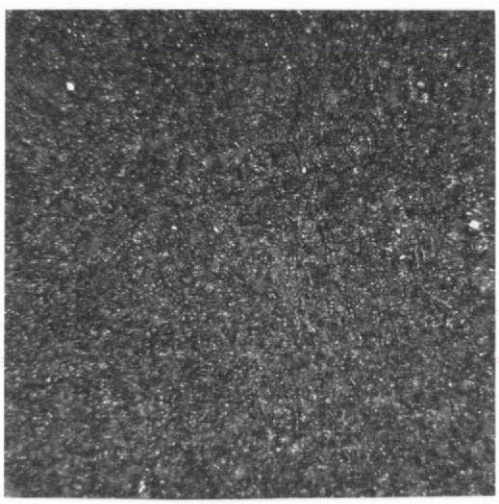

c. MICROPHOTOGRAPH, 200X
(70 a/o Al PACK, 900°C)

*FIG. 1. SURFACE APPEARANCE OF NiAl COATING ($AlF_3$ ACTIVATED PACK)*

TABLE II

Variation of Surface Composition with Time

(10:90 metal:filler ratio)

| Time - hrs. | Surface Composition - a/o Al | | | | | | |
|---|---|---|---|---|---|---|---|
| | 85 a/o Al pack | | | 100 a/o Al pack | | | |
| | 1093°C | 1093* | 800 | 1093 | 1000 | 900 | 800 |
| 2 | ——— | 50.67 | 40.05 | ——— | 60.30 | 62.16 | 59.53 |
| 5 | 46.64 | 49.29 | 44.56 | ——— | ——— | 56.72 | 60.66 |
| 10 | 48.02 | 49.78 | 45.51 | ——— | 52.90 | 53.26 | 61.02 |
| 20 | 47.48 | 49.09 | 44.97 | ——— | 53.35 | 57.01 | 60.87 |

* Retort conditioned with pure Al pack

It is significant that specimens coated in the 85 a/o Al pack emerged with surface a/o Al less than 50. This is lower than surface Al concentrations obtained on specimens coated in a 70 a/o Al pack with a 50:50 metal:filler ratio (Table I). Therefore, the metal:non-metal ratio apparently is significant in, at least, the high Al packs. A somewhat greater variability of surface concentration with time is also evident, although the trend is not clear. The data for the 100 a/o Al pack is particularly interesting. At 1093 the samples were partially melted and no meaningful data were obtained. At 1000 and 900°C the $Ni_2Al_3$ phase was found at the surface of samples treated for 2 hrs., but only NiAl appeared on samples treated for longer times, while at 800°C the $Ni_2Al_3$ phase appeared at all times.

In the case of pure Al packs, the results again cannot be reconciled in terms of loss of Al from the pack. The pack must remain at unit activity as it delivers Al to the Ni surface. Above $\sim$ 850°C, the solid phase with highest Al content is $Ni_2Al_3$, and in the absence of a significant activity gradient in the vapor phase, this is expected to form. Below 850°C, formation of $NiAl_3$ is to be expected as per the phase diagram. The formation of $NiAl_3$ has not been observed

at all and $Ni_2Al_3$ formation seems to be determined by both temperature and time for a given pack of fixed metallic content. Fig. 2(a) illustrates the as coated appearance of sample in 85 a/o Al pack (metal/filler : 10:90). The surface looks very similar to one coated in 58 a/o Al pack (metal to filler ratio of 50:50). This is to be expected since the surface compositions are nearly equal in both cases. Figs. 2(b) and 2(c) are photomicrographs of samples coated in pure Al packs at 1093°C. Samples were melted partially. Fig. 2(b) contains bands of almost pure Al and the matrix is $Ni_2Al_3$ (58.7 a/o Al). Fig. 2(c) is different area of the same sample. Here NiAl grains (51.5 a/o Al) are present. Figs. 3(a) and 3(b) illustrate the as coated $Ni_2Al_3$ appearance and sectioned layer respectively. Original polishing scratch marks on Ni are visible on this surface. This is manifestation of predominant Al diffusion inside the sample. $Ni_2Al_3$ layer is very clean, free of pores or inclusions.

Pure Al (100% Al pack) runs with decreased metal to filler ratio of 4:96 w/o were also conducted in the temperature range of 800 to 1100°C. The results from these runs are shown in Table III.

TABLE III

Variation of Surface Composition with Time in 100 a/o Al Pack

(4:96, metal:filler ratio)

| Time - hrs. | Surface Composition a/o Al | | | |
|---|---|---|---|---|
| | 1093°C | 1000°C | 900°C | 800°C |
| 2 | 51.34 | 52.46 | 64.26 | 57.79 |
| 5 | 50.41 | 52.04 | 53.94 | 57.57 |
| 20 | 50.74 | 54.16 | 53.34 | 59.47 |

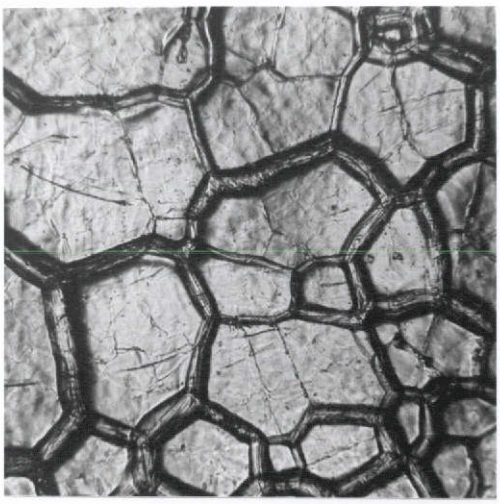

a. MICROPHOTOGRAPH, 200X
(85 a/o Al PACK, 1093°C)

b. MICROPHOTOGRAPH, 200X
(100 a/o Al PACK, 1093°C)

c. MICROPHOTOGRAPH, 200X
(100 a/o Al PACK, 1093°C)

*FIG. 2. SURFACE APPEARANCE OF COATING IN $AlF_3$ ACTIVATED HIGH Al PACK. (METAL TO FILLER RATIO OF 10:90 w/o)*

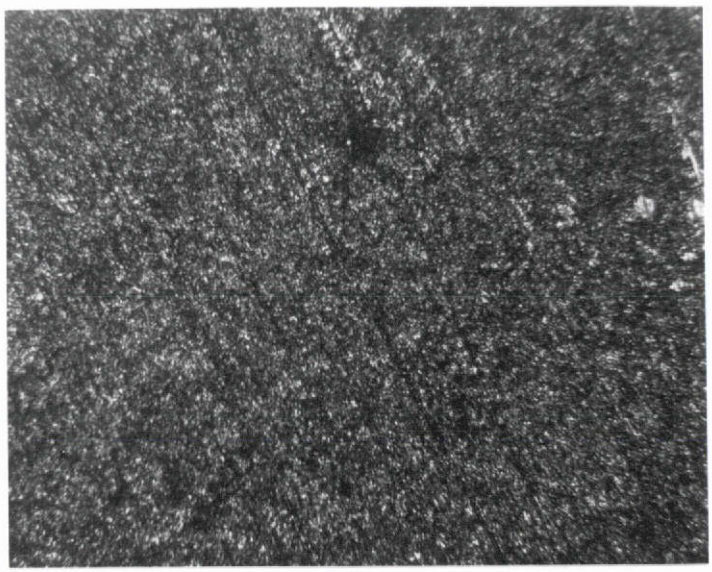

a. As COATED SURFACE APPEARANCE, 200X

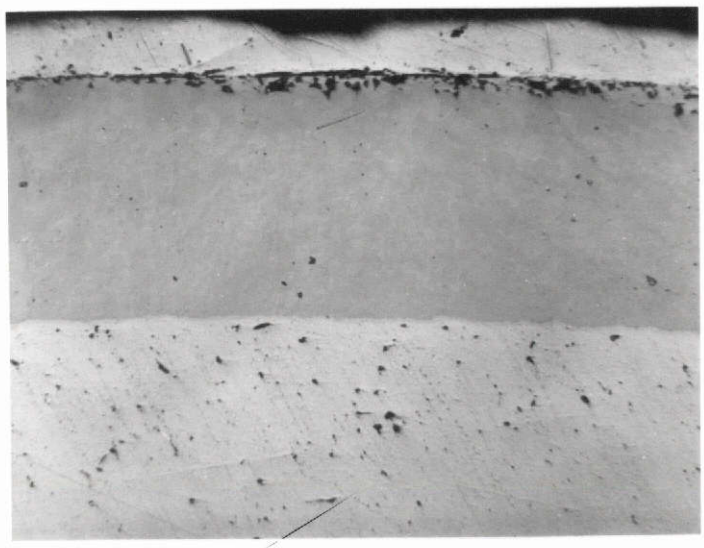


b. LAYER STRUCTURE, 200X

FIG. 3. $Ni_2Al_3$ COATING IN $AlF_3$ ACTIVATED PURE Al PACK, AT 800°C (METAL TO FILLER RATIO OF 10:90 w/o)

While the edges of some of the specimens at 1093 (and 1000°C) were melted, it was possible to obtain surface compositions which proved to lie entirely within the NiAl phase range. The surface compositions were somewhat lower than those obtained at 1000°C using a 10:90 w/o metal:filler ratio (Table II). At 900°C, $Ni_2Al_3$ appeared on the 2 hour specimen but NiAl on the five and twenty hour specimens, similar to the results with the 10:90 pack, except that the surface compositions of the five and twenty hour specimens were a little lower in Al. At 800°C the surface phase was $Ni_2Al_3$, but of slightly lower Al content than that obtained at 800°C in the 10:90 metal:filler ratio pack. In all cases the surface concentration reached a high value of Al content quickly, and, with exception of the 900°C runs, did not change much with time thereafter.

In pure Al packs (unit activity), the surface composition at 1093°C ($\sim$ 51 a/o Al) is lower than at 900°C ($\sim$ 54 a/o Al). Also, $Ni_2Al_3$ is formed at 800°C and in early times at 900°C. Only NiAl formation is favored at 1000°C and 1093°C in spite of the fact that the pack Al activity is unity.

The evident lack of equilibrium between the pack and the specimen surface in high Al packs indicates that the kinetics of the coatings process is not controlled exclusively by solid state diffusion in these packs, even though the surface composition remains relatively constant. It appears that the rate of vapor transport, or, conceivably, of surface reaction, is not rapid enough to maintain an equilibrium composition at the surface when the pack Al activity is high. It appears necessary therefore to take the transport and reaction processes in the vapor phase into account, in order to explain the behavior of the high Al packs.

As a starting point we have applied the ingenious theoretical analysis of Levine and Caves[2] to the behavior of our pure Al packs. This model assumes the formation of a zone depleted of Al adjacent to the specimen surface, through which the aluminum halides are transported by gaseous diffusion. (We have observed the

formation of such a depleted zone in pure Al packs). It is assumed also that the surface of the specimen remains at a constant composition, and that the composition of the vapor phase at the specimen surface is determined by conditions of thermodynamic equilibrium at this surface as well as a balance of the inward and outward fluxes of non-metallic atoms, such as the halide atoms.

According to Levine and Caves, the instantaneous flux is given by:

$$\frac{N_{Al}d}{A} = \frac{\sum_{i=1}^{n} D_i (P_i - P_i')}{RT} \tag{1}$$

where $D_i$ and $P_i$ are the diffusivity and partial pressure of the $i^{th}$ aluminum bearing species, and d is the diffusion distance. The amount of Al deposited in $mg/cm^2 sec$, w, is given by:

$$w^2 = \frac{2\rho\varepsilon}{\lambda}\left(\frac{N_{Al}d}{A}\right) 2.7 \times 10^4 t \equiv k_{Al}t \tag{2}$$

where $\varepsilon$ and $\lambda$ are correction factors for pack porosity and pore length, and $\rho$ is the pack Al density in $mg/cm^3$.

The pack reactions considered in our packs were:

$$2\ AlF_3(g) + Al \rightleftarrows 3\ AlF_2(g) \tag{3}$$

$$AlF_2(g) + Al \rightleftarrows 2\ AlF(g) \tag{4}$$

$$AlF_2(g) + HF(g) \rightleftarrows AlF_3(g) + \tfrac{1}{2}\ H_2(g) \tag{5}$$

The interdiffusion coefficients of $AlF_3$, $AlF_2$, AlF and HF gases with $H_2$ were estimated at different temperatures (800°C - 1093°C) using optimized Gilliland Type Equation[3]. Equilibrium partial pressures of the various fluorides and $H_2(g)$ for unit pack Al activity were calculated. Results of these were given in Report #1. Free fluorine gas pressure is $\sim 10^{-15}$ atm at 1093°C. Fluorine, $NiF_2$, etc., need not be considered owing to very low partial pressures. These calculations assume total pressure of 1 atm., which is the case in our open retorts. Using the condition

of fluorine balance at the specimen surface, the equilibrium partial pressures of above fluorides were evaluated for the surface compositions (activity) given in Table III for the case of 4 w/o Al pack. Table IV gives the rate constant values and the calculated and experimentally observed weight gain data.

It can be seen that the calculated weight gain is 5-10 times greater than the observed weight gain at surface compositions of 51* and 54 a/o Al, while the calculated and observed weight gains are nearly alike when surface compositions are 59 and 64 a/o Al. While there are still discrepancies remaining, the preliminary calculations suggest that a transition from solid state to vapor diffusion control is theoretically possible in the surface composition range 50-100 a/oAl in such packs. A more complete set of calculations is being carried out in order to compare rates of solid and gaseous transport over a wider range of conditions.

## III. Effect of Activators on Coating Kinetics

Investigation of the formation of aluminide coatings on pure nickel was continued during this report period. As discussed in the last progress report[1], quite significant differences between the sodium halide activators and the aluminum fluoride activator were found in the weight gain and surface composition data. These appear particularly in the surface compositions of the specimens coated in the lower Al packs, with NaCl and NaI activators. It

---

* The deposition rate constant predicted by Levine and Caves (2) for gaseous transport in an ammonium fluoride activated pack containing 1 wt. % Al to a 50 a/o Al surface is $k_{Al} = 1.7 \times 10^{-8}$ gm$^2$/cm$^4$ sec. We have obtained a much larger value of $k_{Al}$ mainly because of the differences in pack Al content as well as in equilibrium partial pressures of AlF(g) and $AlF_2$(g). Our values of these pressures, based on the presence of $AlF_3$ condensed phase, are given in Report #1. They agree well with Walsh's (6) but differ substantially from those used by Levine and Caves (2).

TABLE IV

Aluminum Deposition Rate Constants ($k_{Al}$) and Weights (W) by Gaseous Diffusion

(4 w/o pack, $AlF_3$ activator)

| 1093°C | | | 900°C | | | | | | 800°C | | |
|---|---|---|---|---|---|---|---|---|---|---|---|
| Surface Composition | | | Surface Composition | | | | | | Surface Composition | | |
| 51 a/o Al | | | 54 a/o Al | | | 64 a/o Al | | | 59a/o Al | | |
| $k_{Al}$ $\frac{gm^2}{cm^4} \cdot \frac{1}{sec}$ | $W_{Th}$ $\frac{gms}{cm^2}$ | $W_{Exp.}$ $\frac{gm}{cm^2}$ | $K_{Al}$ | $W_{Th}$ | $W_{Exp}$ | $k_{Al}$ | $W_{Th}$ | $W_{Exp}$ | $K_{Al}$ | $W_{Th}$ | $W_{Exp}$ |
| | 20 hrs. | 20 hrs. | | 20 hrs. | 20 hrs. | | 2 hrs. | 2 hrs. | | 20 hrs. | 20 hrs. |
| $1.22 \times 10^{-6}$ | 0.42 | 0.04 | $4.6 \times 10^{-7}$ | 0.26 | 0.03 | $1.3 \times 10^{-7}$ | 0.04 | 0.02 | $2.5 \times 10^{-9}$ | 0.02 | 0.019 |

$K_{Al}$ = Rate Constant

$W_{Th}$ = Theoretical Weight Gain ($W_{Th}^2 = k_{Al} \times \text{Time}$)

$W_{Exp}$ = Experimental Weight Gain

was suggested that a reason for lower surface concentration and low coating weights might be the lower aluminum halide vapor pressures in sodium chloride and iodide activated packs.

During this report period experiments with sodium halide activators were extended to higher Al:Ni ratio packs and the study of effect of the activators on coating kinetics was further extended to include ammonium halides. The partial pressures of aluminum halides generated with $NH_4Cl$ and $NH_4I$ activators can be much higher than those with sodium halide activators due to the absence of a condensed phase. Because of high gaseous pressures with these activators the experiments were generally performed in sealed retorts.

A. Experimental Procedure

Details of the experimental procedure have been already described in progress report I [1]. The experiments were carried out with packs of Al:Ni ratios varying from 45 a/o Al to 100 a/o Al. The time and temperature of coating were 20 hrs. and 1093°C respectively for all experiments. With sodium fluoride activated packs open retorts with slide-fitting covers were used, whereas with NaCl, NaI, $NH_4I$ and $NH_4Cl$ as activators. arc-welded sealed retorts were employed because the vapor pressures of these activators are appreciable at coating temperature. Vapor pressures of the sodium halides are, for example:

| Activator | Vapor Pressure in atm. at 1093°C |
|---|---|
| NaF | .0017 |
| NaCl | .0346 |
| NaI | .152 |

The pack powder was dried to remove any absorbed moisture before welding the retort shut since the presence of moisture in the pack tended to cause the build-up of excessively high pressures. Before carrying out the coating experiments, the retorts were preconditioned for 72 hrs. at 1093°C with a pack of the

same composition as to be used during coating. This was done to minimize the loss of aluminum from the pack to the retort walls during the actual coating experiment. With NaF, Na and NaI, the amount of activator was 4 w/o of the pack but in case of $NH_4Cl$ and $NH_4I$, the amount of activator was reduced to 0.5 w/o of the pack in order to keep the gas pressures at a reasonable level in the sealed retorts. The following tables give the theoretically calculated partial pressures of various gases at two different pack aluminum activities, for $NH_4Cl$ and $NH_4I$ activators with .5 w/o of activator at 1093°C.

TABLE V(a)

Equilibrium Partial Pressure of Gases in $NH_4Cl$

Activated Packs at 1093°C (in atm.)

| $a_{Al}$ | $P_{AlCl(g)}$ | $P_{AlCl_2(g)}$ | $P_{AlCl_3(g)}$ | $P_{Al_2Cl_6}$ | $P_{HCl}$ | $P_{H_2}$ | $P_{Total}$ |
|---|---|---|---|---|---|---|---|
| 1 | .630 | 8.656 | 5.658 | 0.034 | 0.102 | 105.45 | 120.530 |
| .001 | $7.7\times10^{-3}$ | 1.293 | 7.76 | 0.170 | 0.806 | 105.45 | 115.48 |

TABLE V(b)

Equilibrium Partial Pressure of Gases in $NH_4I$

Activated Packs at 1093°C (in atm.)

| $a_{Al}$ | $P_{AlI(g)}$ | $P_{AlI_3(g)}$ | $P_{Al_2I_6}$ | $P_{HI}$ | $P_{H_2}$ | $P_{Total}$ |
|---|---|---|---|---|---|---|
| 1 | 3.15 | 3.177 | $8.379\times10^{-3}$ | 0.113 | 25.3 | 31.638 |
| .001 | $3.37\times10^{-2}$ | 3.89 | $1.256\times10^{-2}$ | 0.488 | 25.3 | 29.72 |

As shown in Table V the total pressure is theoretically quite high with both $NH_4Cl$ and $NH_4I$ activators. However, the $H_2$ probably quickly diffuses through the walls of the retort. The partial pressures of aluminum halides are much higher than those generated with sodium halides as activators. Thus, although the percentage of activator in the pack is reduced, an increase in gas transport rates would be expected.

In experiments with high Al: Ni ratio packs the metallic content of the pack was reduced to 10 w/o in order to avoid an excessive amount of liquid phase.

B. Results and Discussion

The weight gains and surface compositions of the coatings are summarized in tables VI and VII. As clear from table VI, the weight gains after coating with NaF as activator are in reasonably good agreement, although slightly higher than those from $AlF_3$ activated packs. Pack particles sticking on the coating surface may be responsible for higher weight gains.

TABLE VI

Weight Gain Data for Various Activators, in $gm/cm^2$

(20 hrs. at $1093^oc$)

| a/o Al in Pack | NaF | NaCl | NaI | $AlF_3$ | $NH_4Cl$ | $NH_4I$ |
|---|---|---|---|---|---|---|
| | | | For 50 w/o metallic content in pack | | | |
| 45 | 0.0198*<br>0.02138 | 0.0025* | 0.0020* | | 0.0020 | 0.0013 |
| 50 | 0.0207*<br>0.0222 | 0.0050* | 0.0022* | 0.0157 | 0.0199 | 0.0016 |
| 55 | 0.0205* | 0.0166*<br>0.0028 | 0.0188 | 0.0163 | 0.0199 | 0.0037 |
| 60 | 0.0197* | 0.0189* | 0.0207* | 0.0169 | 0.0185 | 0.011 |
| 70 | 0.0189 | 0.0198 | 0.155 | 0.0195 | 0.0224 | 0.0211 |
| | | | For 10 w/o metallic content in pack | | | |
| 85 | 0.0171 | 0.0117 | 0.007 | 0.0176 | 0.012 | 0.0097 |
| 100 | .0633<br>0.0491 | 0.0178 | 0.0155 | | .0238 | 0.0189 |

* The results of coating experiments reported in progress report #2 (1)

TABLE VII

Surface Composition of Coated Ni Specimen in a/o Al

(at 1093°c for 20 hrs.)

| a/o Al in Pack | NaF | NaCl | NaI | $AlF_3$ | $NH_4Cl$ | $NH_4I$ |
|---|---|---|---|---|---|---|
| | | | For 50 w/o metallic content in pack | | | |
| 45 | 44.03*<br>41.3 | 12.19* | 5.16 | 41.62 | ------ | ------ |
| 50 | 47.52*<br>44.0 | 39.37 | 6.23 | 47.43 | 44.3 | ------ |
| 55 | 49.13* | 48.24* | 49.07* | 47.83 | 43.2 | ------ |
| 60 | 49.56* | 52.27* | 49.71* | 49.11 | 48.7 | 48.0 |
| 70 | 49.1 | 48.5 | 48.2 | 54.43 | 52.5 | 48.6 |
| | | | For 10 w/o metallic content in pack | | | |
| 85 | 48.5 | ------ | ------ | 47.48 | 45.0)<br>39.6) | 50.1 |
| 100 | 46.5<br>48.8 | 51.69 | 51.61 | ------ | 53.0 | 52.57 |

* The results of coating experiments reported in the progress report II.

The coatings formed with NaF activated packs are quite similar in appearance to those formed with $AlF_3$ activated packs. The surface compositions with NaF activated packs (Table VII) are also comparable to those with $AlF_3$ activated packs, except for some discrepancies at higher aluminum packs. An unexplained peculiarity in the weight gain data is that, as shown in Tables VI and VII, the weight gain of coated specimens in a pure Al, NaF activated pack is much higher than the normal weight gain, whereas corresponding surface composition is lower than expected. This result was

obtained in two experiments, but the reason for the inconsistency is not clear. The aluminide coatings formed in NaCl, NaI, $NH_4Cl$ and $NH_4I$ activated packs differed in various degrees with those formed in $AlF_3$ activated packs. Most normal in appearance were the coatings deposited in the $NH_4Cl$ activated packs. While the amount of Al deposited in the 45 a/o Al packs is very low as reflected in weight gain data, in higher Al:Ni ratio packs the weight gain in $NH_4Cl$ activated packs is slightly higher than in fluoride activated packs. In general, the surface compositions of specimens coated in $NH_4Cl$ activated packs are slightly lower than those coated in $AlF_3$ activated packs but not greatly different.

The aluminide coatings formed with NaCl, NaI and $NH_4I$ activated packs differed more substantially from those with $AlF_3$ activated packs regarding surface appearance, weight gain and surface composition. As clear from weight gain data with NaCl, NaF and $NH_4I$ activated packs, very little coating was formed at 45 and 50 a/o Al. A similar conclusion is reflected from the surface composition data (Table VII). The surfaces of specimens coated in these packs did not exhibit the usual smooth and brigh appearance of NiAl but possessed a dull etched appearance. This structure is illustrated by area "A" of Figure 4a.

The aluminide coatings deposited in higher aluminum packs with NaCl, NaF and $NH_4I$ activators had an irregular surface appearance. Some areas of these specimens are typified by area "A" of Figure 4a. Such areas are light yellow in color with the so-called "etched" appearance. As shown in the scanning electron photomicrograph of Figure 4b, these areas consisted of faceted grains, which explains the directional reflection and "etched" appearance. A cross-section of the specimen showing the layer structure under area "A" is shown in Figure 4c. It may be seen that a thin irregular layer of compound has formed at such sites with much porosity.

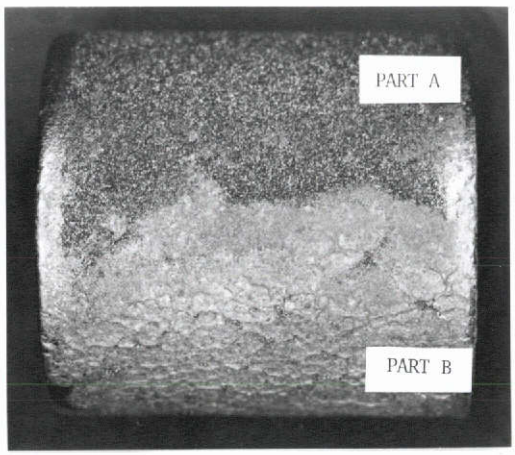


a) Macrophotograph, 8X

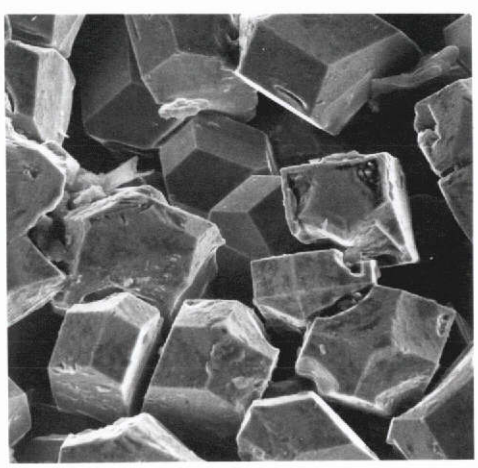

b) SEM photograph of surface at PART A, 600X

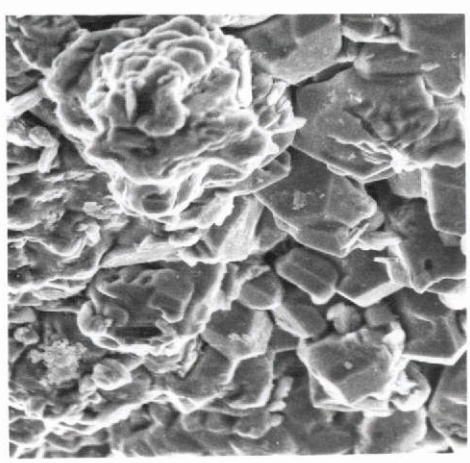

c) SEM photograph of surface at PART B, 1200X

Fig. 4 Surface and layer structure of Ni specimen coated in 60 a/o Al: 40 a/o Ni pack with $NH_4I$ activator for 20 hours at 1093°C

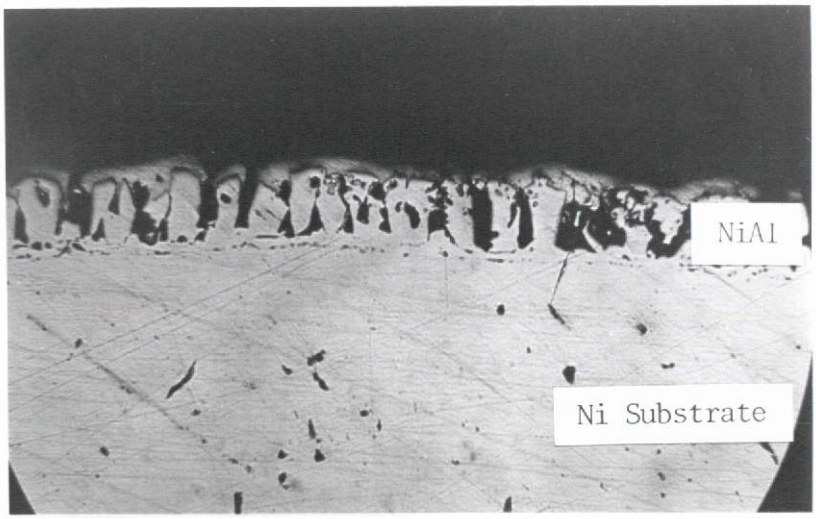


d) Layer structure under PART B, 150X

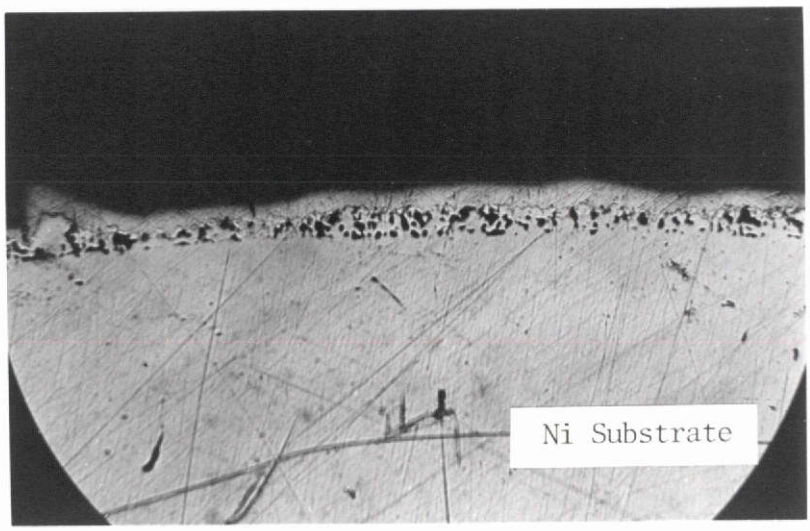


e) Layer structure under PART A, 150X

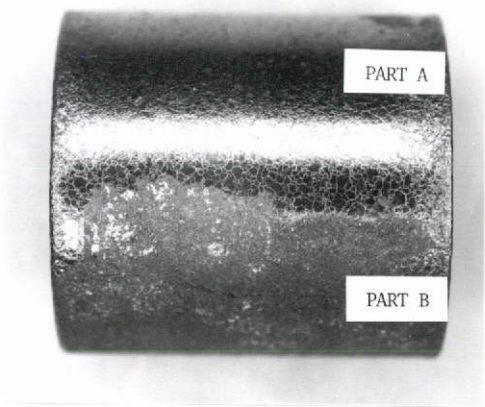


a) Macrophotograph, 8X

b) SEM photograph of surface at PART A, 500X

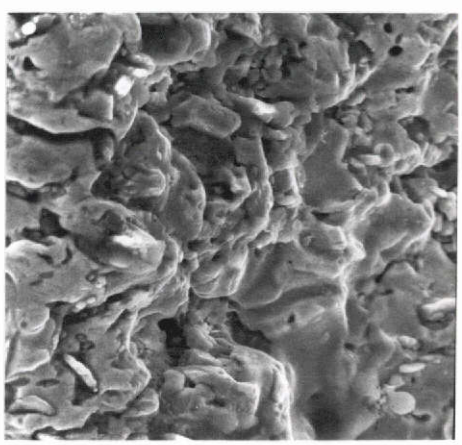

c) SEM photograph of surface at PART B, 1200X

Fig. 5 Surface and layer structure of Ni specimen coated in 100 a/o Al pack with NaCl activator for 20 hours at 1093$^{O}$C

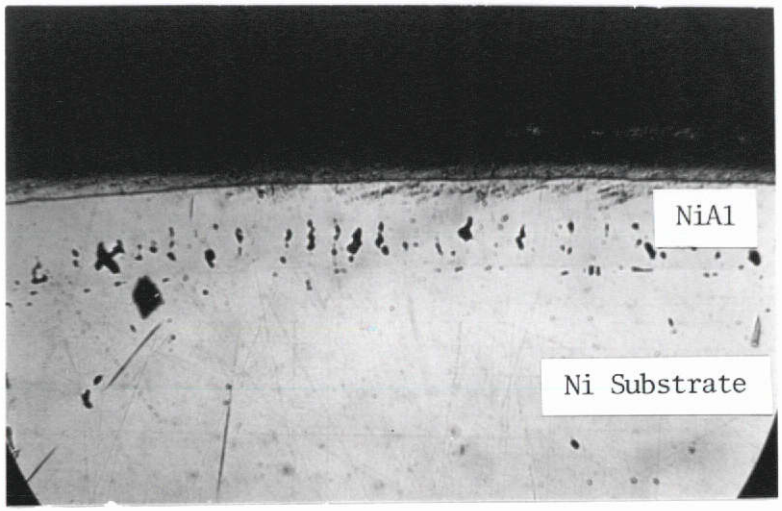


d) Layer structure under PART A, 150X

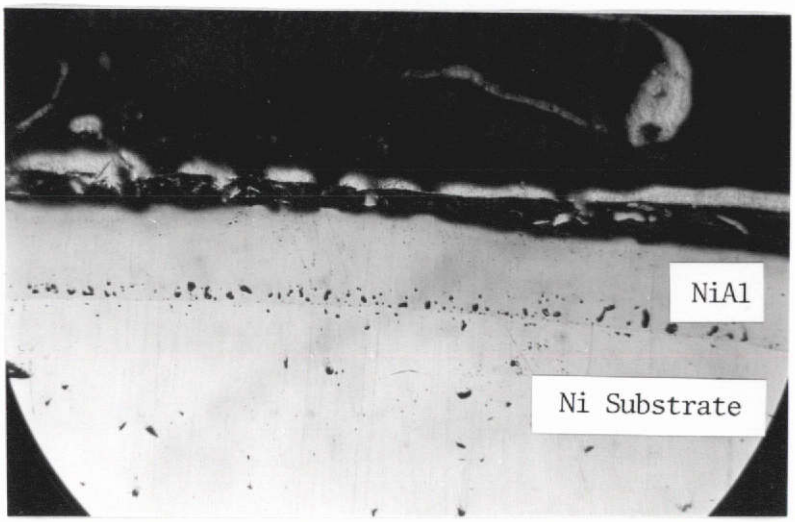


e) Layer structure under PART B, 150X

Area "B" of the specimen shown in Figure 4a consists of a light blue non-reflecting surface. The scanning electron photomicrograph of this area is given in Figure 4c and the layer structure shown in Figure 4d. Individual grains of NiAl seem to have grown separately upward in the formation of this layer, with voids between grains appearing as porosity in the layer. Another type of surface is illustrated by area "B" of Figure 5a. This usually occurs near areas of bright NiAl coating, and appears to be a deposit of pack material over the normal NiAl layer. This is confirmed by the fact that the electron beam was deflected during microprobe measurements, indicating the presence of non-metallic particles on the coating surface. The layer structure beneath this surface is shown in Figure 5e, and the scanning electron photomicrograph in Figure 5c. This differs very much from the NiAl coating shown in Figure 5b.

Inconsistencies between surface compositions and weight gains evident in Tables VI and VII can now be explained on the basis of irregularity of surface structure. For example, the weight gain with the 60 a/o Al, $NH_4I$ activitated pack is lower than with the 70 a/o Al, $NH_4I$ activitated pack, whereas the measured surface compositions are approximately the same. With so much variation in coating structure and thickness over the surface of these specimens, it is difficult to obtain representative values, and the interpretation of the weight gain and composition data for the higher Al packs activated with NaCl, NaI, and $NH_4I$ is open to doubt in some instances. In spite of this difficulty the evidence seems to be clear that the iodide activators are less effective than the chloride, and the chloride less effective than the fluoride.

## IV. Correlation of Layer Growth Rates with Diffusivities in the Solid

In Progress Reports 1 and 2, we presented the methods of calculation as well as theoretical and experimental results with respect to growth rates of binary

multiphase coatings. Growth rate calculations can be carried out with the help of exact, analytical relationships. when the interdiffusion co-efficient in each phase is concentration-independent. In many ordered phases and intermetallic compounds, the interdiffusion co-efficient may vary strongly with composition, as has been found for NiAl in our diffusion studies. For such cases, numerical solution of the diffusion equation has to be performed. In this report, we will briefly review, and compare the applicability of the closed-form and numerical solutions, eliminate an inconsistency regarding the coordinate system that introduced some inaccuracy in previous calculations, and present the results obtained to date.

A. Concentration-independent Interdiffusion Co-efficient

Aluminide coatings on specimens of pure nickel are formed by exposing them to a gas containing aluminum and some non-metallic constituents. This is generated from a pack of controlled aluminum activity, such that the surface phase is NiAl, and the surface composition remains constant with time. The specimen expands due solely to a gain in solute atoms. Because of this expansion, the surface of the specimen is displaced, and should not be taken as the origin, as in previous reports. The original, or Matano interface is located by the equalization of areas method as shown in Figure 6. Under these conditions, all two-phase interfaces, including the surface, move away from the Matano interface parabolically with time, conveniently expressed as follows:

$$X_s = -2\gamma_s\sqrt{\tilde{D}_\beta t} \qquad \text{---- (1)}$$

$$X_a = 2\gamma_a\sqrt{\tilde{D}_\beta t} \qquad \text{---- (2)}$$

$$X_b = 2\gamma_b\sqrt{\tilde{D}_\beta t} \qquad \text{---- (3)}$$

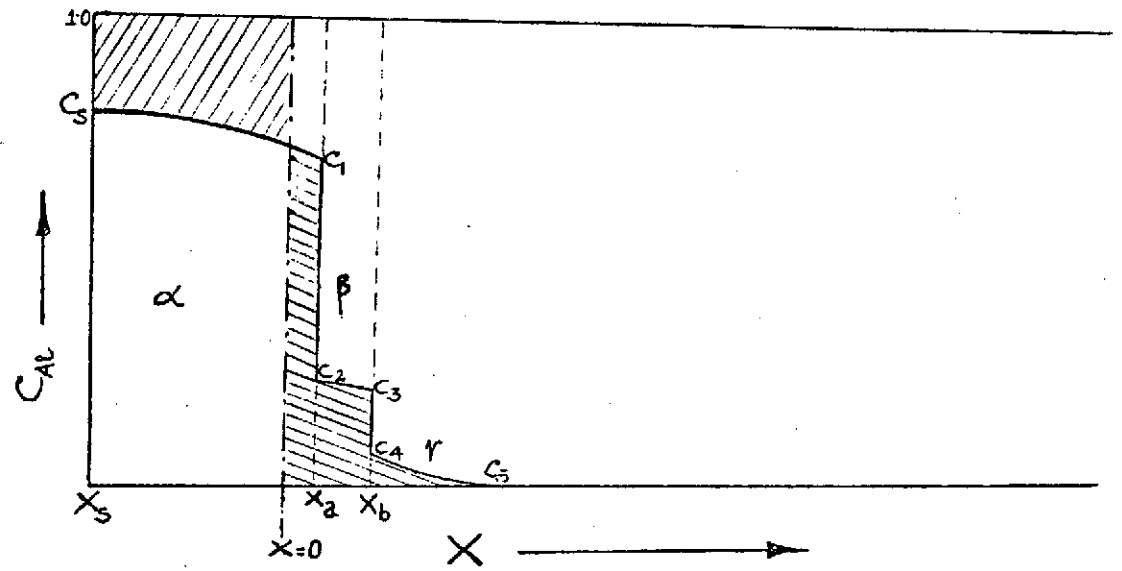


Figure 6: Location of the original interface (x=0) for a semi-infinite binary vapor-solid diffusion couple

The problem is to calculate the dimensionless growth parameters γs, γa, γb for various surface compositions ($C_S$).

If $\tilde{D}_\alpha$, $\tilde{D}_\beta$, $\tilde{D}_\gamma$ are concentration-independent, the following are the concentration-profiles in α, β and γ phases:

$$C(\alpha) = C_1 + \frac{(C_S - C_1)}{\text{erf}\gamma a\sqrt{D\beta/D\alpha} + \text{erf}\gamma s\sqrt{D\beta/D\alpha}} \left(\text{erf}\gamma a\sqrt{D\beta/D\alpha} - \text{erf}\frac{X}{2\sqrt{D_\alpha t}}\right) \quad \text{---- (4)}$$

$$C(\beta) = C_3 + \frac{(C_2 - C_3)}{\text{erf}\gamma b - \text{erf}\gamma a} \left(\text{erf}\gamma b - \text{erf}\frac{X}{2\sqrt{D\beta t}}\right) \quad \text{---- (5)}$$

$$C(\gamma) = C_5 + \frac{(C_4 - C_5)}{1 - \text{erf}\gamma b\sqrt{D\beta/D\gamma}} \left(1 - \text{erf}\frac{X}{2\sqrt{D\gamma t}}\right) \quad \text{---- (6)}$$

Furthermore, the interface velocities can be related to interface material balance, by means of equations 7, 8 and 9 below. These will yield three algebraic equations

in $\gamma s$, $\gamma a$ and $\gamma b$, upon substitution of the appropriate derivatives from equations 1 through 6. They have to be solved simultaneously for $\gamma s$, $\gamma a$, $\gamma b$ for any given surface composition $C_S$. It can be shown that this solution will also satisfy the Matano condition.

| Interface | Velocity Equation | Unknown Parameters |
|---|---|---|
| Vap.-Solid $X_S$ | $\frac{dX_s}{dt} = \frac{1}{1.0-C_s}(J^V - J^\alpha) = \frac{1}{1-C_s}(0+\tilde{D}_\alpha \frac{\partial C(\alpha)}{\partial X})X_s$ ---- (7) | $\gamma s$, $\gamma a$ |
| $\alpha$-$\beta$ $X_A$ | $\frac{dX_a}{dt} = \frac{1}{C_1-C_2}(-\tilde{D}_\alpha \frac{\partial C(\alpha)}{\partial X} + \tilde{D}_\beta \frac{\partial C(\beta)}{\partial X})X_a$ ---- (8) | $\gamma s$, $\gamma a$, $\gamma b$ |
| $\beta$-$\gamma$ $X_B$ | $\frac{dX_b}{dt} = \frac{1}{C_3-C_4}(-\tilde{D}_\beta \frac{\partial C(\beta)}{\partial X} + \tilde{D}_\gamma \frac{\partial C(\gamma)}{\partial X})X_b$ ---- (9) | $\gamma a$, $\gamma b$ |

B. Concentration-dependent Interdiffusion Co-efficients

We have experimentally determined the interdiffusion co-efficients in NiAl, $Ni_3Al$ and the nickel-rich terminal solid solution. While the diffusivities are constant, within experimental error, in both $Ni_3Al$ and the terminal solution, the interdiffusion co-efficient not only varies with concentration in NiAl, but it shows a minimum at around 48.5 a/o Al. The diffusivity data at 1093°C, analyzed from a specimen having a surface composition of 52.5 a/o Al, are given in Figure 7.

To compute layer thicknesses of NiAl and $Ni_3Al$ for any surface composition, temperature and coating time, we can still make use of all equations of scheme (A), except equation (4). This analytic solution for NiAl is no longer valid for a

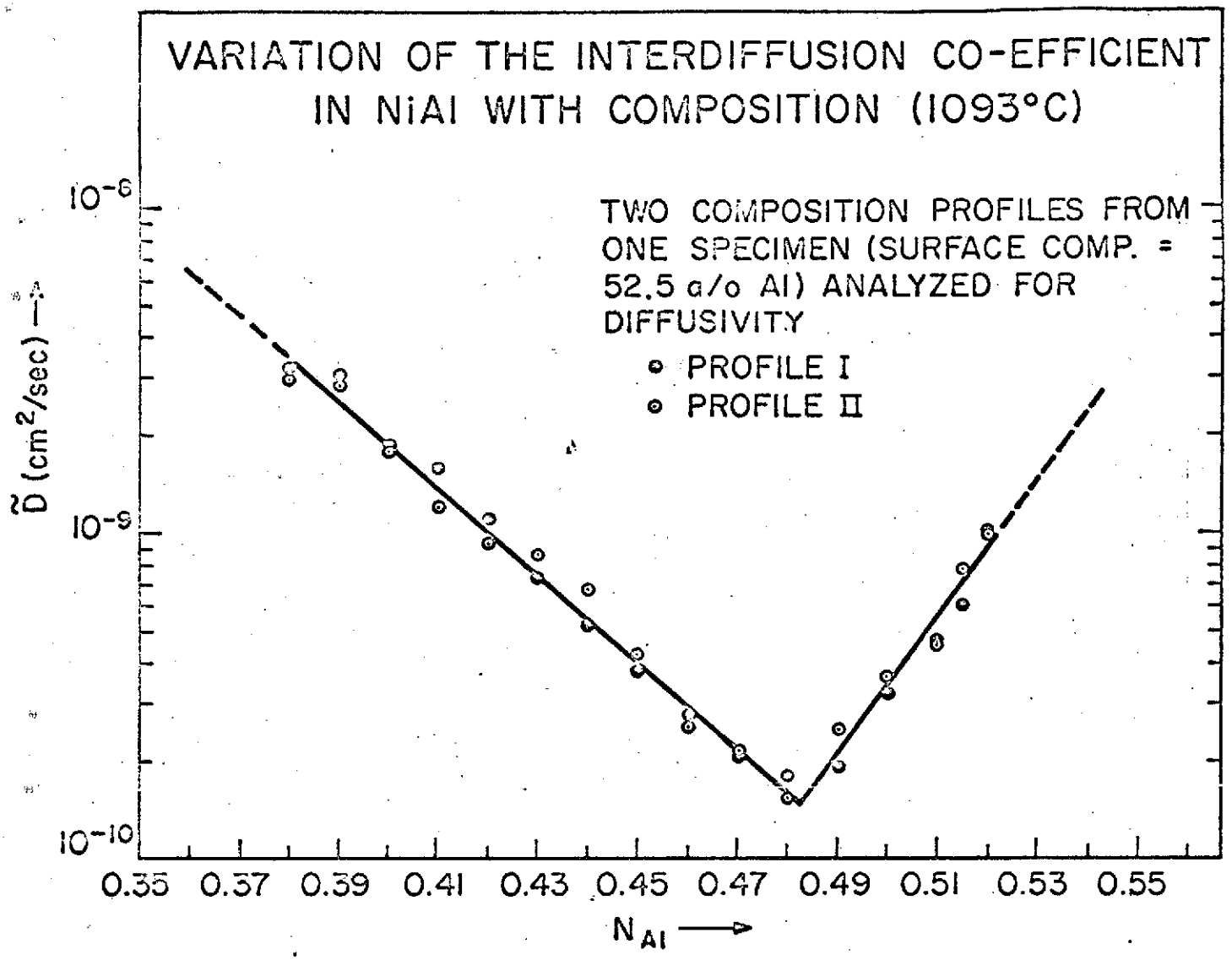


Figure 7

## INTERDIFFUSION CO-EFFICIENTS AT 1093°C

**NiAl**

$$\tilde{D}\,(cm^2/sec) = 4.332.\ 10^{-4}\ EXP\,(-30.847.\ N_{Al});\quad 0.358 \le N_{Al} < 0.483$$

$$\tilde{D}\,(cm^2/sec) = 1.121.\ 10^{-20}\ EXP\,(48.274.\ N_{Al});\quad N_{Al} > 0.483$$

**$Ni_3Al$**

$$\tilde{D} \approx 1.8 \times 10^{-10}\ cm^2/sec$$

**Ni-Al Solid Soln.**

$$\tilde{D} \approx 2.0 \times 10^{-10}\ cm^2/sec$$

concentration-dependent interdiffusivity ($\tilde{D}_\alpha = D_o Exp(-\beta.C)$ in NiAl). The diffusion equation has to be solved numerically:

$$\frac{\partial C(\alpha)}{\partial t} = \frac{\partial}{\partial X}\left\{\tilde{D}_\alpha \frac{\partial C(\alpha)}{\partial X}\right\} \qquad (10)$$

With new variables:

$$Z = \frac{X}{2\gamma_a\sqrt{\tilde{D}_\beta t}}$$

and $$Y = Exp(-\beta \cdot C)$$

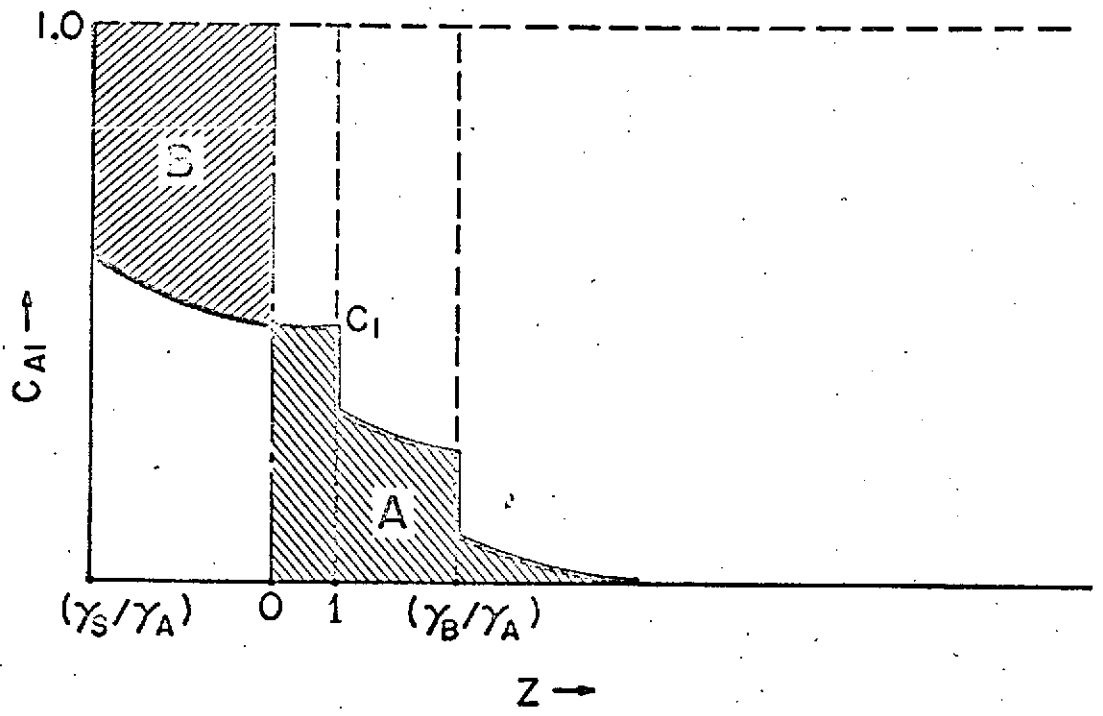


Figure 8: Solution for Concentration-dependent Diffusivity.

(10) is transformed to an ordinary differential equation:

$$Y \frac{d^2Y}{dZ^2} + \frac{2\gamma_a^2 \tilde{D}\beta}{D_0} \cdot Z \cdot \frac{dY}{dZ} = 0 \qquad (11)$$

To solve (11), the following steps are carried out:

1. Equation (9) contains only $\gamma_a$ and $\gamma_b$. Choose any $\gamma_b$ and compute $\gamma_a$ from this.

2. Rewrite (8) in terms of the new variable Z:

$$\left.\frac{dc(\alpha)}{dZ}\right|_{Z=1} = \frac{2\tilde{D}\beta \cdot \gamma A}{\tilde{D}_\alpha|_{Z=1}} \frac{(C_3-C_2)\ \exp(-\gamma_a^2)}{\sqrt{\pi}(\mathrm{erf}\gamma_B - \mathrm{erf}\gamma_a)} - (C_1-C_2)\gamma_a$$

compute

$$\left.\frac{dY}{dZ}\right|_{Z=1} = -\beta \cdot \mathrm{Exp}(-\beta \cdot C_1) \cdot \left.\frac{dC(\alpha)}{dZ}\right|_{Z=1}$$

3. The initial conditions for the transformed differential equation (11) in NiAl are:

$$\left.\begin{aligned} Y_1 &= \mathrm{Exp}(-\beta \cdot C_1) \\ \frac{dY}{dZ} &= \text{known} \end{aligned}\right\} \quad \text{at } Z = 1$$

The differential equation is solved by the method of finite differences for decreasing values of Z, and continued to the negative side of the Z-axis, until the two areas A and B are equal. The latter locates the specimen surface. From the values of Y and Z at the surface, $C_S$ and $\gamma S$ are obtained. Thus, the problem is solved in an indirect way - a surface composition, and the NiAl and $Ni_3Al$ layer thicknesses that it will give rise to , are calculated, starting from a chosen value of $\gamma B$. This can be repeated to cover a wide range of surface compositions. The

method is illustrated schematically in Figure 8.

C. Results

Figure 9 shows that the concentration profile in and the layer thickness of NiAl, calculated by the numerical procedure described above, compare very well with the electron micro-probe analyzed profile for a specimen with 52.5 a/o surface composition.

Theoretically calculated layer thicknesses as a function of the surface composition have been plotted in Figure 10. These have been compared with layer thickensses obtained from the concentration-independent diffusivity scheme, (A). In the latter, the integrated composition average diffusion co-efficient for NiAl has been used:

$$\bar{D}(\alpha) = \frac{1}{C_s - C_1} \int_{C_1}^{C_s} \tilde{D}_{\alpha}(C)\,dC$$

For each surface composition ($C_s$), $\bar{D}$ has a different value, but then it is assumed constant for all compositions between $C_s$ and $C_1$.

| $C_s$(a/0 Al) | $\bar{D}(\alpha)$ ($x10^9 cm^2/sec$) |
|---|---|
| 36.2 | 6.52 |
| 37.5 | 5.42 |
| 40.6 | 3.63 |
| 42.2 | 3.02 |
| 46.4 | 2.05 |
| 49.2 | 1.65 |
| 52.5 | 1.44 |

The resulting layer thickensses are accurate (Figure 10), but the concentration profiel (error-function solution) departs considerably from the actual one, as can be

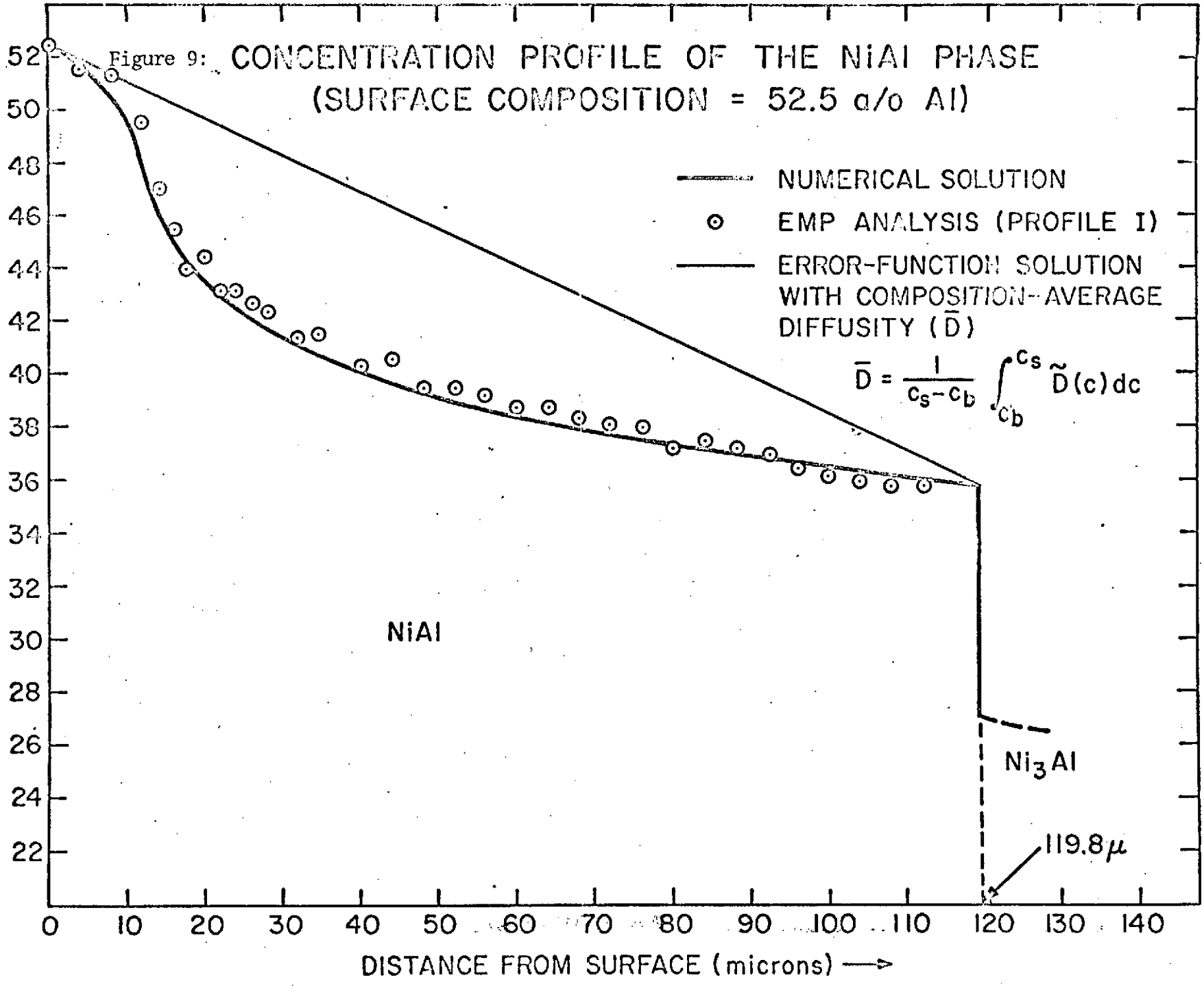


Figure 9:

Figure 10

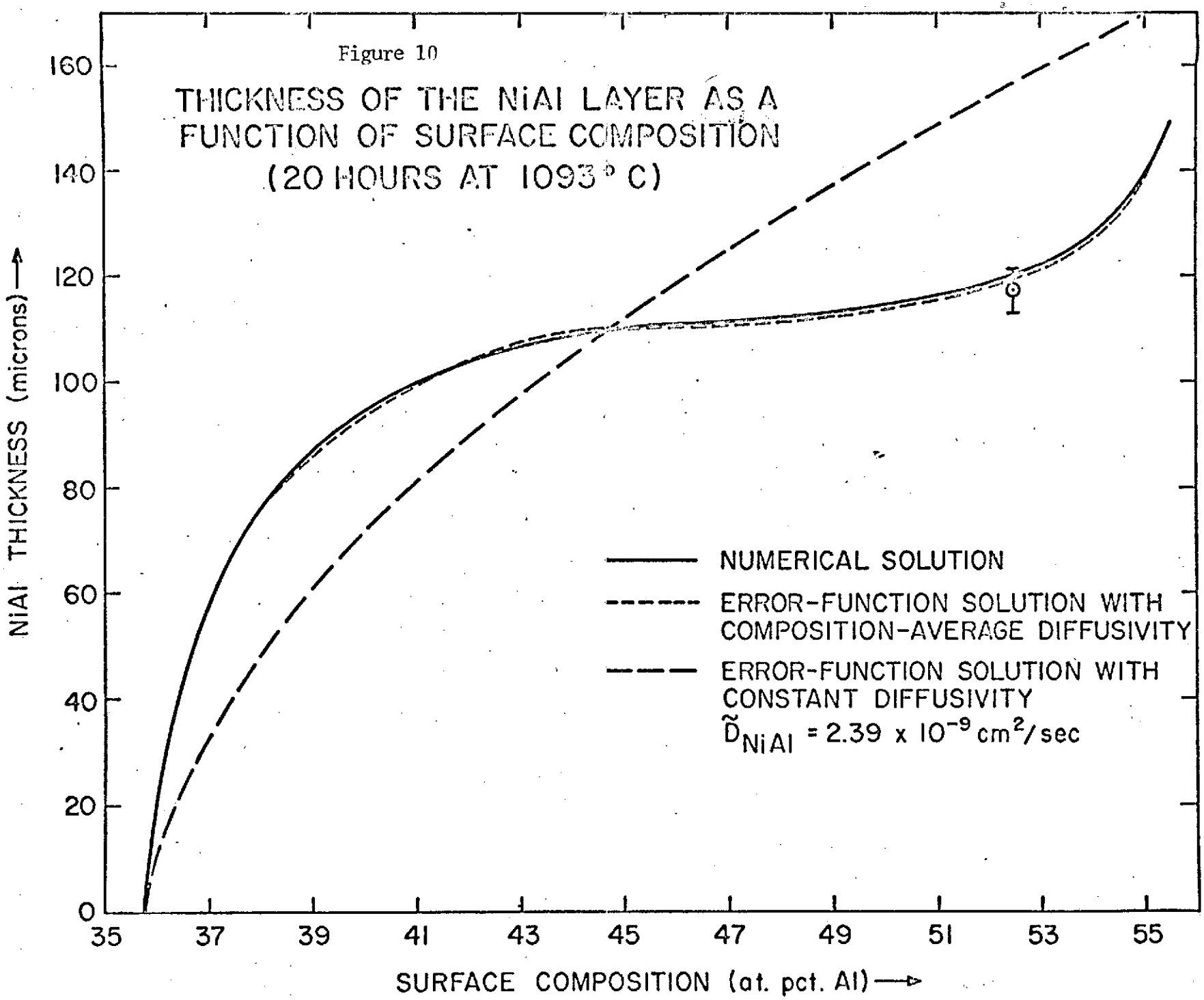
THICKNESS OF THE NiAl LAYER AS A FUNCTION OF SURFACE COMPOSITION (20 HOURS AT 1093° C)
NiAl THICKNESS (microns) ⟶
SURFACE COMPOSITION (at. pct. Al) ⟶
0
20
40
60
80
100
120
140
160
35
37
39
41
43
45
47
49
51
53
55
NUMERICAL SOLUTION
ERROR-FUNCTION SOLUTION WITH COMPOSITION-AVERAGE DIFFUSIVITY
ERROR-FUNCTION SOLUTION WITH CONSTANT DIFFUSIVITY
$\tilde{D}_{NiAl} = 2.39 \times 10^{-9}$ cm$^2$/sec

Figure 11

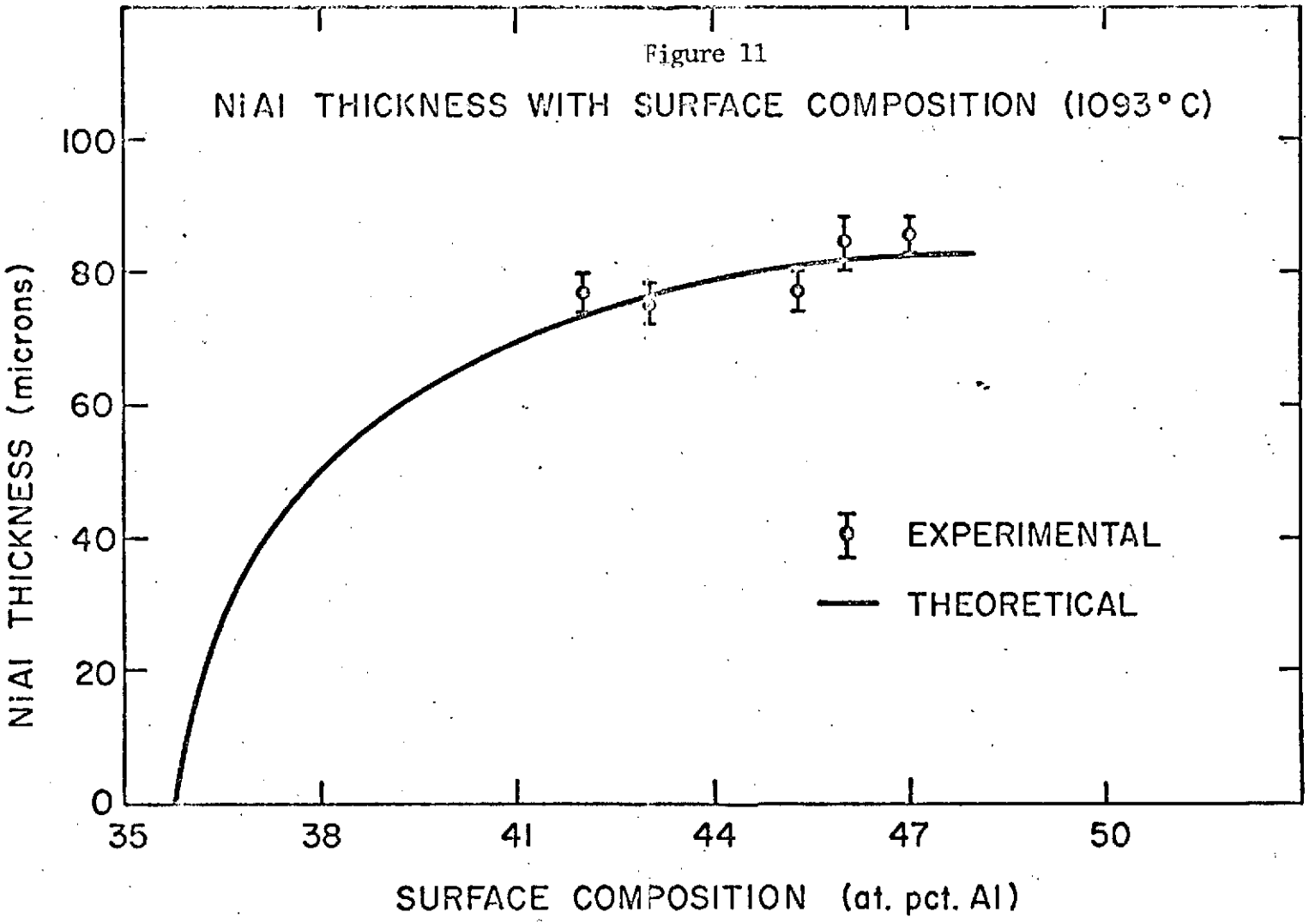
NiAl THICKNESS WITH SURFACE COMPOSITION (1093° C)
NiAl THICKNESS (microns)
0
20
40
60
80
100
35
38
41
44
47
50
SURFACE COMPOSITION (at. pct. Al)
EXPERIMENTAL
THEORETICAL

seen in Figure 9, for the 52.5 a/o Al surface composition. As a generalization, whenever the interdiffusion co-efficient in any phase is concentration-dependent, this integrated average diffusivity in conjunction with an error-function solution, can be used to calculate growth rates, although the correct concentration profile, if required, should be calculated numerically.

It is possible to compute an integrated composition average diffusivity only if $\tilde{D}$ is known as a function of concentration in the entire homogeneity range of a phase. Very often, such data are lacking, and a single value of the interdifusivity is used to characterize the phase. To demonstrate that this will generally lead to considerable errors, we have calculated NiAl layer thicknesses (Figure 10) from Scheme (A), using an NiAl diffusivity of $2.39 \times 10^{-9}$ $cm^2/sec$.

A comparison has been made in Figure 11 between experimental and theoretical NiAl layer thicknesses resulting from a 20 hour coating treatment at 1093°C, for surface compositions upto 48a/oAl, for which we have representative data.

We will conclude by pointing out that the numerical method can also be applied when phases in the interior of the coating have diffusivities varying with concentration, exponentially or otherwise.

## V. Oxidation Versus Coating-Substrate Interdiffusion

Depletion of aluminum from protective aluminide coatings, and their consequent failure have generally been attributed to alternate oxide formation and spallation, under thermal cycling and the highly dynamic conditions of the engine environment, with metal temperature in the range of 1400 to 1800°F. Theoretical estimates of the rate of coating degradation by interdiffusion (1), as well as recent experimental studies on commercial superalloys (4), have indicated that coating-substrate interdiffusion may play an important role in degradation of aluminide coatings during service.

In static oxidation, a stable adherent $Al_2O_3$ forms on the surface of the coating, inhibiting further oxidative degradation. However, diffusive degradation can cause the underlying NiAl layer to be depleted in Al, and converted eventually to non-oxidation-resistant phases. For binary nickel-aluminide coatings (NiAl-$Ni_3Al$-matrix) on pure Ni, this diffusion process is simple in that, after a relatively short transient period during which the concentration gradient in the NiAl layer is homogenized, the $Ni_3Al$ grows continuously at the expense of the NiAl layer. This effect is demonstrated in Figure 12, by annealing in air for 25 hours at 2000°F, an aluminized specimen having a thin $Ni_3Al$ layer, which has resulted in

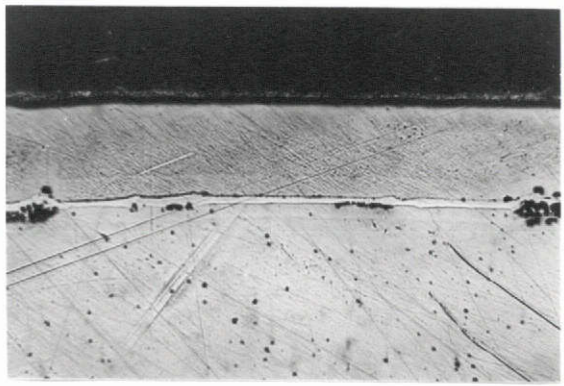

a) As-coated Specimen, 200X

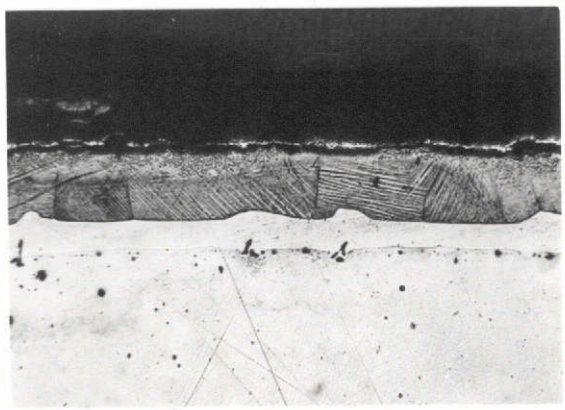

b) Specimen annealed in air for 25 hours at 2000$^{O}$F after coating, 200X

Fig. 12. Coating Degradation by Interdiffusion

the broadening of the latter. The NiAl layer in the annealed specimen shows evidence of martensitic transformation, indicating (5) that it has been depleted in Al. The kinetics of this diffusion process can be followed experimentally by gravimetry, metallography, microprobe analysis and x-ray diffractometry of the specimen surface, and, for binary coatings such as those on pure Ni and Co, amenable to mathematical analysis. For the purpose of experimentally investigating the diffusion kinetics, annealing should be done in an inert atmosphere to eliminate any interference from oxidation.

Our future efforts in this area will be directed towards a computer analysis of diffusive degradation, using diffusivity data for the Ni-Al system, as well as a detailed experimental study, at least at two temperatures - 1800 and 2000°F. The kinetics of the process is too slow to make experimental studies below 1800°F practicable, but based on diffusivity data, behavior at lower temperatures can be inferred.

The relative importance of diffusion and oxidation, under conditions of thermal cycling, as competing mechanisms of degradation of aluminide coatings on highly alloyed practical superalloys is a complex subject. The initially formed protective $Al_2O_3$ spalls off due to thermal cycling, and it may be that repeated formation and spallation of product oxides consumes the Al in the coating far more rapidly than interdiffusion, under actual operating conditions. But according to a degradation model put forward by Smialek and Lowell (4), interdiffusion is still important in that the depletion of Al from NiAl (to a composition below ~40a/o Al) apparantly makes it more oxidation-prone. This happens because the product of oxidation changes from pure $Al_2O_3$ to a mixture of $Al_2O_3$, NiO and complex Ni-Al spinels, which form and spall at a faster rate. Thus, interdiffusion triggers a latter catastrophic oxidation process. In view of this apparent importance of interdiffusion, we believe that a detailed theoretical and experimental examination

of this process, under suitably idealized conditions, is warranted.

## VI. Future Work

### A. Kinetics of Pack Aluminization

The most recent data obtained with $AlF_3$ activated packs indicate that, while at low Al: Ni pack ratios solid state diffusion is the rate controlling process during aluminization, the situation is more complex at high Al: Ni ratios. At high ratios the surface composition of the coating appears to assume a value which, although invariant with time, is not in equilibrium with the bulk pack composition. In order to explain this observation it seems necessary to take the mass transfer processes in the gas into consideration and a more concentrated effort on the theory of gaseous diffusion in the pack is planned for the immediate future. Fortunately, the model of Levine and Caves (2) furnishes an excellent basis for such considerations, at least so far as pure Al packs are concerned, and this will be applied to our pack conditions. For packs containing lower Al: Ni ratios it is possible that a somewhat different model is needed, and an effort will be made to develop a suitable theory for gaseous transport in such packs.

In view of the evident lack of equilibrium in high Al, fluoride activated packs between coating surface and pack, it is planned to carry out further investigations of the variation of surface composition with time in order to clarify the role of vapor phase to solid phase diffusion in such packs. It is desired, in particular, to extend our measurements to earlier coating times, and also to investigate the influence of varying pack metallic content, which, according to Levine and Caves model, is an important variable with respect to Al transport in the vapor phase. Finally, a limited exploration of the aluminization of pure cobalt is planned, in order to explain certain peculiarities in the mode of coating growth on Co which have already been observed (1).

With regard to the role of varying activator, it seems clear from our data, as well as that of Levine and Caves (2), that significant differences exist among the activators, and it is likely that gaseous diffusion plays a more important role in packs activated with iodide and chloride than with fluoride. In continuation of the work underway, first an effort will be made to better characterize the structural anomalies observed, particularly with iodide activated packs, by further microprobe and metallographic studies. Second, it is felt that a more concentrated study of the behavior of the various activators over a more limited range of conditions is needed in order to adequately define the differences in properties. For this reason it is planned to carry out a detailed comparison of the activators using Ni specimens in a 100a/o Al pack. Use of such a pack not only simplifies the experiments by eliminating the pretreatment step, but also affords the possibility of a direct comparison of experimental results with the predictions of Levine and Cave's theory. The variation of surface composition with time will be determined at one or two temperatures and the usual structural data will also be obtained.

B. Correlation of the Rate of Formation and Structure of Coatings with Diffusional Properties

The mathematical problem of calculating rates of layer growth as a function of surface composition, allowing for variable diffusity in the intermetallic phases, has essentially been solved, and future work in this phase of the program will be concentrated on obtaining more complete information about diffusion parameters in the Ni-Al and Co-Al systems. Considerable data are already available for the NiAl system, but further information is needed about the variation of $\tilde{n}$ and $D_{Ni}/D_{Al}$ in NiAl with composition. Such information is being obtained by microprobe and

marker movement studies using pack-aluminized specimens. Work has also been initiated to obtain necessary diffusivity values for the intermediate phases in the Co-Al system, relevant to the aluminization of cobalt-based alloys.

D. Oxidation Vs. Coating-Substrate Interdiffusion

The outstanding problem which remains to be solved is obtaining a mathematical method to predict coating-substrate interdiffusion rates which allows for the complex initial distribution of the coating components as well as the variation of diffusivity with composition. It is planned to conduct a more concentrated effort on this problem in the immediate future. Experimental studies of coating-substrate interdiffusion will also be continued, to obtain data for comparison with theoretical predictions.

When coating-substrate interdiffusion rates have been adequately defined, an assessment of the relative importance of oxidation and coating-substrate interdiffusion as mechanisms of degradation of aluminide coatings will be made using oxidation test data available in the literature.

## REFERENCES

1) B. Gupta, A. Sarkhel, R. Sivakumar, L. Seigle, First and Second Progress Reports, 6/1/72-5/31/73 and 6/1/73-11/30/73, NASA Research Grant NGR-33-015-160

2) S.R. Levine and R.M. Caves, NASA Technical Report TMX-71423, 1973

3) R.H. Perry and C.H. Chelton, "Chemical Engineer's Handbook", McGraw-Hill, 1973

4) J.L. Smialek and C.L. Lowell, NASA Tm E-7590 (1973)

5) J.L. Smialek, Met. Trans. 2 (1971) 913

6) P.N. Walsh, in "Chemical Vapor Deposition" (Fourth International Conference), ed. by G.F. Wakefield and J.M. Blocher, Jr., The Electrochemical Society, Inc., N.J. (1973), 147